

Luminescence Characteristics and Electronic Levels of Eu(III) in the *N,N*-Dimethyl-diphenyl-phosphinamide (DDPA) Adduct of Europium Perrhenate

S. RAM

*Advanced Centre for Materials Science, Indian Institute of Technology,
Kanpur-208016, India*

AND S. K. SINHA*

*Department of Chemistry, Indian Institute of Technology,
Kanpur-208016, India*

Received December 18, 1985; in revised form May 12, 1986

Optical absorption and emission spectra (1200–200 nm) of $\text{Eu}(\text{ReO}_4)_3 \cdot 2\text{DDPA}$ are measured between 77 and 650 K. Based on a C_2 symmetry of the Eu(III) ion, a group theoretical analysis has been carried out and tentative assignments of 5D_J and 7F_J energy levels and their Stark splitting are made. The emission spectra measured with various Ar^+ laser lines exhibit prominent fluorescence exclusively from 5D_0 to 7F_J levels. The relative intensities of the 5D_J emissions exhibit a temperature dependence showing a continuously decreasing intensity for the $J \geq 1$ states. The 5D_0 state remains only a fluorescence state at higher temperatures (above ~ 450 K). For $J \geq 1$, the excited Eu(III) ions in these states decay by a combination of radiative transitions to the 7F_J levels and nonradiative processes operative within the 5D_J manifold. © 1987 Academic Press, Inc.

Introduction

The adducts of lanthanides with *N,N*-dimethyl-diphenyl-phosphinamide (DDPA) are stable and crystallize out in different structures (1, 2). Recently, Vicentini and Machado (3) have synthesized the $\text{Ln}(\text{ReO}_4)_3 \cdot 2\text{DDPA}$ isomorphous series with $\text{Ln} = \text{La}-\text{Tb}$ and $\text{Ln}(\text{ReO}_4)_3 \cdot 3\text{DDPA}$ with $\text{Ln} = \text{Dy}-\text{Lu}$, Y. The "effective" symmetry of these chromophores have not been conclusively determined. The Ln(III) electronic energy levels and their J -level split-

ting are very sensitive to the local symmetry, coordination, and crystal field offered by the nearest neighbors (4, 5). The splitting pattern and intensity distribution within $^5D_J \leftrightarrow ^7F_J$ transition regions can provide information about ligand field structure and symmetry. Moreover, the luminescence properties of lanthanides can be substantially modified by the presence of impurity ions and/or radiation-induced defects as well as by the phonon frequencies of the host lattices (6–9). This may be useful for characterizing the materials for laser applications (10–12).

The absorption spectrum of the europium adduct shows a broad UV absorption due to

* The author to whom correspondence should be addressed.

the DDPA ligand and sharp Eu(III) lines in the visible region. The Eu(III) ion also exhibits the $4f \rightarrow 4f$ transitions in the UV region (13), but these usually get masked into the strong DDPA absorption. These transitions, however, can be utilized to populate the Eu(III) levels of the visible region as the former (UV) transitions are easily excited through the DDPA absorptions. This would lead to the efficient laser emissions from 5D_J levels with the emitted radiation lying in the visible to near infrared. Moreover, among the trivalent lanthanide ions, Eu(III) is especially useful as an optical probe of crystal-field symmetry and radiative transition properties (14). The ground state (7F_0) and the principal emitting state (5D_0) of this ion are nondegenerate, and the spectra remain uncomplicated even in low-symmetry ligand environments. Thus, a study of the Eu(III) ions is of clear interest in any study of the electronic structures of the lanthanide complexes. In this investigation, we report a detailed analysis of the optical absorption and fluorescence spectra associated with the possible $^7F_J \leftrightarrow ^5D_J$ ($J = 0-6$, and $J = 0-4$) transitions of Eu(III) in the $\text{Eu}(\text{ReO}_4)_3 \cdot 2\text{DDPA}$ adduct at different temperatures between 77 and 650 K.

Experimental

The $\text{Eu}(\text{ReO}_4)_3 \cdot 2\text{DDPA}$ was prepared by a method reported elsewhere (3). Its optical absorption (1200–200 nm) from the crystalline powder and single crystal was measured between 77 and 650 K on a Cary-17D spectrophotometer. X-ray diffraction patterns recorded for the powder samples (using a Rich–Seifert Isodebyeflux 2002 diffractometer with filtered $\text{CuK}\alpha$ radiation) at three different temperatures, viz, 77, 300, and 650 K do not differ appreciably from one another. This confirms that the $\text{Eu}(\text{ReO}_4)_3 \cdot 2\text{DDPA}$ adduct is stable and retains the same crystal structure between 77 and 650 K. The fluorescence spectra

were measured on a Ramalog 1403 spectrophotometer equipped with a Spectra-Physics Model 165 Ar^+ laser. The measurements were made using the various Ar^+ laser lines for the excitations in the visible region. This provided a comparison of the Eu(III) fluorescence excited from different 5D_J levels as well as an identification of Raman and fluorescence processes. The low-temperature control was achieved using a homemade dewar, with liquid nitrogen used as the coolant. An electric heater assembly fitted with the dewar was employed for the high-temperature (above 300 K) measurements.

Results and Discussion

Electronic Absorption Spectra

The electronic absorption spectrum of $\text{Eu}(\text{ReO}_4)_3 \cdot 2\text{DDPA}$ exhibits the characteristic sharp bands of Eu(III) in the 600- to 400-nm region. Intense and structureless bands involving the $\pi \rightarrow \pi^*$ transitions of the DDPA group appear in the 400- to 200-nm region and mask the weak Eu(III) absorptions (15, 16). All crystal-field components of the $^7F_0 \rightarrow ^5D_{0,1,2}$ bands between 580 and 460 nm get resolved in the spectra at 77 K. A typical absorption spectrum (600–400 nm) measured at room temperature (300 K) is shown in Fig. 1. Some vibronic bands associated with the electronic transitions are accompanied by blue-shifted broad bands. These are marked by the circled plus sign \oplus . The band position and oscillator strength of the principal band groups assigned for a few low-lying energy transitions are given in Table I. The oscillator strengths of the bands have been calculated using the integral area under the absorption curves (for details, see Feuerhelm *et al.* (17)). Their values so obtained for the $^7F_0 \rightarrow ^5D_J$ ($J = 0-4$) transitions in Eu(III) systems are of particular interest in elucidating the electric/magnetic dipole characters and

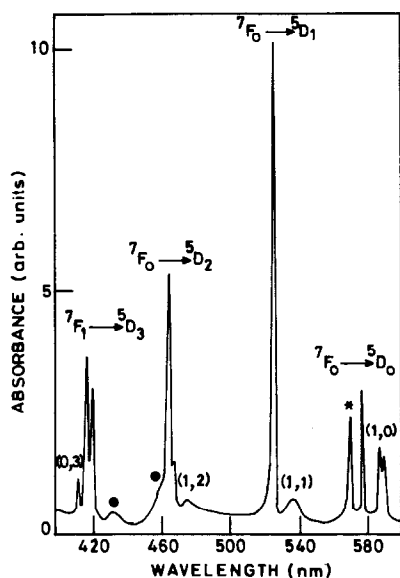


FIG. 1. Absorption spectrum (600–400 nm) of the $\text{Eu}(\text{III})$ ion in $\text{Eu}(\text{ReO}_4)_3 \cdot 2\text{DDPA}$ at 300 K. (*) Absorption of Re^{4+} , (\oplus) vibronic bands.

hence the $4f \rightarrow 4f$ radiative transition probabilities. Among these transitions, only ${}^7F_0 \rightarrow {}^5D_1$ satisfies the magnetic dipole selection rules ($\Delta J = 0, \pm 1$, with $J = 0 \leftrightarrow J' = 0$) in an intermediate coupling scheme (18). The ${}^7F_0 \rightarrow {}^5D_{2,4}$ transitions are believed to be primarily electric dipole in character. Their intensities are therefore strongly dependent on crystal-field effects. The ${}^7F_0 \rightarrow {}^5D_3$ transition has a mixed character (magnetic dipole intensity usually to first order and electric dipole intensity to second order), whereas the remaining ${}^7F_0 \rightarrow {}^5D_0$ transition is rigorously forbidden for any magnetic/electric dipole or electric quadrupole transition. However, this latter transition generally appears (though with small intensity) for the noncentrosymmetric europium compounds due to the J -level mixings. The intensity (oscillator strength) distribution within the ${}^7F_0 \rightarrow {}^5D_J$ transitions of the $\text{Eu}(\text{ReO}_4)_3 \cdot 2\text{DDPA}$ adduct shown in Fig. 1 is consistent with these predictions. Only the ${}^7F_0 \rightarrow {}^5D_1$ band, as an exception, reveals somewhat larger intensity than ex-

pected for a magnetic dipole transition. We have also studied the electronic absorption spectra of $\text{EuCl}_3 \cdot 6\text{H}_2\text{O}$ and $\text{Eu}(\text{SO}_4)_3 \cdot 8\text{H}_2\text{O}$, and similar results for the ${}^7F_0 \rightarrow {}^5D_1$ transition have been noted. Sage *et al.* (19) have measured the absorption and magnetic circular dichroism intensities in $\text{EuCl}_3 \cdot 6\text{H}_2\text{O}$ showing no evidence of the presence of electric dipole/electric quadrupole character, if any, in this transition.

Perhaps a more striking result of the absorption measurements has been observed for a thermally excited ${}^7F_1 \rightarrow {}^5D_3$ band group at ~ 420 nm. It exhibits an intensity ~ 70 times that of the ${}^7F_0 \rightarrow {}^5D_3$ transition excited from the ground state (7F_0) at ~ 300 K. The intensity increases exponentially in

TABLE I
PRINCIPAL ABSORPTION BANDS OF $\text{Eu}(\text{III})$ IN
 $\text{Eu}(\text{ReO}_4)_3 \cdot 2\text{DDPA}$ OBSERVED AT 300 K

Wavelength (nm)	Oscillator strength ($f \times 10^6$)	Transitions
590.0 (16,950)	0.023	${}^7F_1 \rightarrow {}^5D_0$
588.0 (17,007)		
578.4 (17,289)		
570.0 (17,544)*		
536.0 (18,656)		
525.0 (19,048)	0.50	${}^7F_0 \rightarrow {}^5D_1$
472.0 (21,186)	0.010	${}^7F_1 \rightarrow {}^5D_2$
465.0 (21,505)	0.35	${}^7F_0 \rightarrow {}^5D_2$
464.0 (21,552)		
459.0 (21,786) \oplus		
432.0 (23,148) \oplus	—	Vibronic bands
420.0 (23,895)	0.34	${}^7F_1 \rightarrow {}^5D_3$
416.0 (24,038)		
412.0 (24,272)		
393.0 (25,445)		
384.0 (26,042)		
381.0 (26,247)	2.5	${}^7F_0 \rightarrow {}^5G_{2,3,4}$
377.0 (26,525)		
365.0 (27,397)	5.0	${}^7F_0 \rightarrow {}^5D_4$

Note. Transition energies (in cm^{-1}) are written in parentheses.

* Absorption band of Re^{4+} .

\oplus Vibronic band as marked in Fig. 1. Here, Stark splittings are omitted.

the excitation of ${}^7F_1 \rightarrow {}^5D_3$ bands and decreases in the ${}^7F_0 \rightarrow {}^5D_3$ excitation following the Boltzmann population distribution with temperature increases between 77 and 650 K. The bands of the latter transition almost disappear at ~ 650 K. Thermally excited bands to the ${}^5D_{0-2}$ levels have also been noted (cf. Table I), but these are not so pronounced. The appearance of the thermally excited Eu(III) bands, as in the present case, is not very surprising. Several examples (20–22) in this series have been reported wherein the absorptions excited for 7F_1 levels of the Eu(III) ion revealed an even stronger intensity than those excited for the 7F_0 level. The crystal-field-induced electric dipole characters of the involved levels and their pertinent selection rules are generally responsible for these features.

High-resolution spectra of the ${}^7F_0 - {}^5D_1$ (525 nm) and ${}^7F_0 - {}^5D_2$ (464 nm) transitions show very clear crystal-field splittings into three and five Stark components, respectively. This indicates a sufficiently low site symmetry (most probably C_{2v} , C_2 , C_s , or C_1) of Eu(III) in this adduct as the $2J + 1$ -fold degeneracy of each 5D_1 and 5D_2 is com-

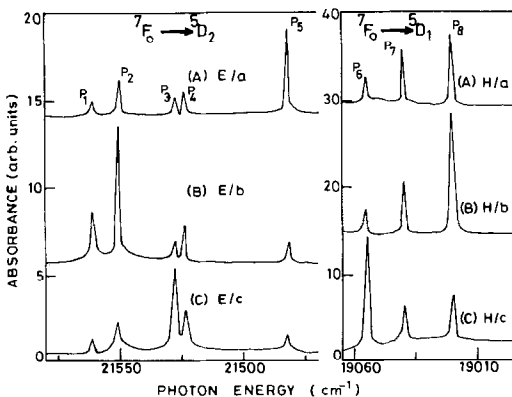


FIG. 2. Polarized absorption spectra of the ${}^7F_0 \rightarrow {}^5D_1$ and ${}^7F_0 \rightarrow {}^5D_2$ bands of the Eu(III) ion at ~ 77 K. The electric vector E for the ${}^7F_0 \rightarrow {}^5D_2$ transition and the magnetic vector H for the ${}^7F_0 \rightarrow {}^5D_1$ transition were kept parallel to a , b , and c crystal axes in (A), (B), and (C), respectively.

TABLE II
ABSORPTION LINES OF 7F_0 TO ${}^5D_{2,1,0}$ MULTIPLETS OF Eu(III) IN THE $\text{Eu}(\text{ReO}_4)_3 \cdot 2\text{DDPA}$ ADDUCT. THE ASSIGNMENT OF THE EXCITED STATE LEVELS OF THE TRANSITIONS IS MADE BY C_s POINT GROUP SYMMETRY

Line	Line energy (cm^{-1})			Assignment	C_s symmetry
	77 K	300 K	650 K		
P_1	21,561	21,560	21,575	${}^7F_0(\Gamma_1) \rightarrow {}^5D_2$	Γ_2
P_2	21,552	21,552	21,560		Γ_1
P_3	21,527	21,530	21,537	${}^7F_0(\Gamma_1) \rightarrow {}^5D_1$	Γ_2
P_4	21,524	21,527	21,532		Γ_1
P_5	21,482	21,485	21,490	${}^7F_0(\Gamma_1) \rightarrow {}^5D_0$	Γ_1
P_6	19,055	19,058	19,060		Γ_1
P_7	19,040	19,045	19,046		Γ_2
P_8	19,020	19,022	19,030	${}^7F_0(\Gamma_1) \rightarrow {}^5D_0$	Γ_2
P_9	17,289	17,290	17,295		Γ_1

pletely removed. We have also measured the polarized absorption spectra of these crystal-field transitions (Stark lines). The results obtained for the different geometrical configurations of a thin single crystal of the $\text{Eu}(\text{ReO}_4)_3 \cdot 2\text{DDPA}$ adduct are consistent with each other. The polarized spectra measured with electric vector (E) incident parallel to the crystal axes a , b , and c are shown in Fig. 2. For the sake of simplicity, the absorption lines of transitions from 7F_0 to Stark levels of ${}^5D_{2,1,0}$ states are numbered as P_1 to P_9 in the order of decreasing energy. The transition energies and symmetry species of P_1 levels obtained at three representative temperatures, viz., 77, 300, and 650 K are given in Table II. The transition ${}^7F_0 \rightarrow {}^5D_1$ as discussed above is a well-known magnetic dipole transition. Its polarization is, therefore, characterized by the orientation of the magnetic vector (H) in the reference light. The spectral features of the Stark lines P_6 , P_7 , and P_8 (${}^7F_0 \rightarrow {}^5D_1$ bands group) in Fig. 2 reveal that these belong to two different symmetry types. The P_6 line exhibits the same intensity in the two orientations $H//a$ and $H//b$ and it differs from that in the $H//c$ orientation. We have assigned this band to a Γ_1 symmetry species in the C_s point group symmetry. Likewise,

the P_7 and P_8 lines are attributed to the Γ_2 symmetry species.

A considerable polarization effect is noted in the P_1 to P_5 lines. This eventually confirms a predominant electric dipole character of the ${}^7F_0 \rightarrow {}^5D_2$ transition. The five (P_1 to P_5) Stark components (in C_s point group symmetry) can be written as

$$\Gamma_{5D_2} = 3\Gamma_1 + 2\Gamma_2.$$

Here, the transition moment for the Γ_1 species lies in a plane defined by the a and b crystal axes and that for the Γ_2 species lies perpendicular to this plane (23, 24). Thus the Stark lines with the Γ_1 species would occur strongly (weakly for the Γ_2 species) in $E//a$ and $E//b$ orientations with a relatively weaker (stronger for the Γ_2 species) intensity in the $E//c$ orientation. The relative intensities as occurred in these five Stark lines change drastically in the different orientations from $E//a$ to $E//c$ (cf. Fig. 2) but do not rigorously follow any specific pattern permissible under a C_s or C_1 site symmetry. The observed features, however, can be better accounted for by a C_{2v} symmetry. The assignments of the lines P_1 to P_5 by this symmetry would be the transitions

$$\Gamma_1({}^7F_0) \rightarrow \Gamma_3, \Gamma_1, \Gamma_2, \Gamma_1, \text{ and } \Gamma_4({}^5D_2),$$

respectively. The line P_1 assigned to the forbidden Γ_3 species may arise in a distorted C_{2v} (to C_2) symmetry. This, however, does not justify an apparent contradiction of different site symmetries concluded for the ${}^7F_0 \rightarrow {}^5D_1$ (C_s) and ${}^7F_0 \rightarrow {}^5D_2$ (C_{2v}) transitions. A correlation diagram of the symmetry species in different symmetry sites is given in Table III.

Fluorescence Spectra

At present, the "effective" symmetry of $\text{Eu}(\text{ReO}_4)_3 \cdot 2\text{DDPA}$ is not understood (3, 25, 26). On the basis of X-ray diffraction studies of this compound, Vicentini and Machado (3) have suggested a C_{4v} symmetry with distortion to C_{2v} . The $\text{Eu}(\text{O})_6$ chro-

TABLE III
CORRELATION DIAGRAMS FOR DIFFERENT SYMMETRY SITES AS PERMISSIBLE FOR THE $\text{Eu}(\text{III})$ ION IN THE $\text{Eu}(\text{ReO}_4)_3 \cdot 2\text{DDPA}$ ADDUCT

Sites Species	C_2	C_{2v}	C_s	C_1
$\Gamma_1(A)$		$\Gamma_1(A_1)$		
		$\Gamma_2(B_1)$	$\Gamma_1(A')$	
$\Gamma_2(B)$		$\Gamma_3^*(A_2)$		$\Gamma_1(A)$
		$\Gamma_4(B_2)$	$\Gamma_2(A'')$	

* Electric dipole forbidden transition. All other transitions are allowed in both the electric dipole and the magnetic dipole (23). Some authors use the notations given in parentheses.

mophore forms a distorted square bipyramid with four oxygens of the two bidentate perchrenate (ReO_4)⁻ ions occupying the equatorial plane at about the same distance. The results of our absorption studies reported here indicate that the complex suffers a still lower symmetry. To deduce more structural information about the complex, we carried out fluorescence studies. The results obtained at 77 K are shown in Figs. 3 and 4. The emission spectrum shown in Fig. 3 displays emissions mainly from the 5D_0 level. The emission intensity is fairly intense, indicating an absence of concentration quenching in $\text{Eu}(\text{ReO}_4)_3 \cdot 2\text{DDPA}$. A sequence of ${}^5D_0 \rightarrow {}^7F_J$ transitions was observed and contained a wealth of fine Stark line structure. The most intense spectral features exhibit sharp lines followed by less intense and relatively broader lines located at slightly lower energies. These broad contours exhibit very little loss of intensity as the temperature rises from 77 to 650 K. The broad features are vibronic in nature and the sharp lines are origin transitions. Assignments for the major peaks shown in Figs. 3 and 4 are summarized in Table IV.

The 5D_0 state of $\text{Eu}(\text{III})$ is nondegenerate

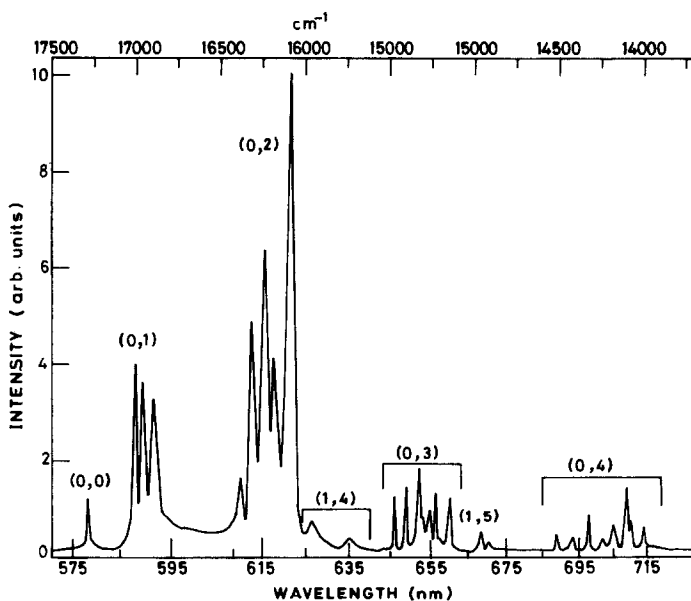


FIG. 3. Fluorescence spectrum of the Eu(III) ion in $\text{Eu}(\text{ReO}_4)_3 \cdot 2\text{DDPA}$ at 77 K with the principal emitting state 5D_0 . $\lambda_{\text{exc}} = 488.0 \text{ nm}$ Ar^+ laser.

and the spectrum ${}^5D_0 \rightarrow {}^7F_J, (0, J')$ remains simple even for low-symmetry environments. The transition ${}^7F_0 \rightarrow {}^5D_0$ in the europium adduct occurred for both the absorption and the emission spectrum. Its

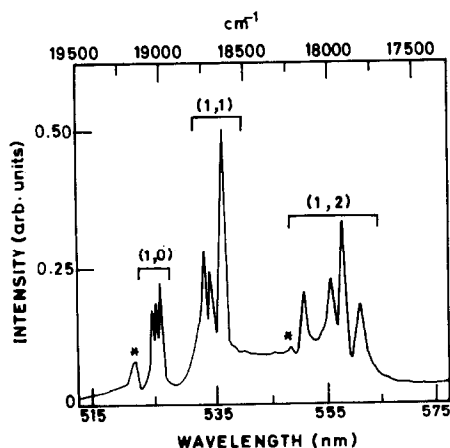


FIG. 4. Fluorescence spectrum of the Eu(III) ion corresponding to that of Fig. 3 with the principal emitting state 5D_1 . * = Vibronic bands.

oscillator strength known for the absorption spectrum thus may be utilized to speculate (assuming the same oscillator strength also in emission) on the oscillator strengths of the remaining $(0, J')$ emissive transitions using their relative emission intensity data. The result so obtained is given in Table V. The line assignments summarized in Table IV follow the selection rules described in the Judd-Ofelt theory (27, 28). The transitions ${}^5D_0 \rightarrow {}^7F_J$ in emission obey essentially the same restrictions as for the ${}^7F_0 \rightarrow {}^5D_J$ transitions in the absorption. Thus the transitions ${}^5D_0 \rightarrow {}^7F_1$ and ${}^5D_0 \rightarrow {}^7F_{2,4,6}$ (predominantly magnetic dipole and electric dipole, respectively, in character) should exhibit appreciable intensities. The other three transitions ${}^5D_0 \rightarrow {}^7F_{0,3,5}$ usually exhibit low intensities independent of ligand field. The magnetic dipole intensities of the ${}^5D_0 \rightarrow {}^7F_{0,3,5}$ transitions occur to first order in the even parity crystal field and the electric dipole intensities to second order (odd parity-even parity state mixing + $J-J'$ mix-

ing). The results of the present investigation are consistent (cf. Fig. 3 and Table V) with these facts. However, the (0, 3) transition exhibits a relatively larger intensity. It is likely due to its large induced electric

TABLE IV

EMISSION LINES OF $\text{Eu}(\text{III})$ IN $\text{Eu}(\text{ReO}_4)_3 \cdot 2\text{DDPA}$
OBSERVED AT 77 K ($\lambda_{\text{exc}} = 488 \text{ nm Ar}^+$ LASER)

Wavelength (nm)	Energy (cm^{-1})	Assignment [$J(i) \rightarrow J'(i)$]
(1, 0) Band		
521.7	19,168	Vibronic
524.8	19,055	1(c)-0(a)
525.2	19,040	1(b)-0(a)
525.7	19,022	1(a)-0(a)
(1, 1) Band		
533.3	18,751	1(b)-1(a)
534.3	18,716	1(b)-1(b)
536.5	18,639	1(b)-1(c)
(1,2) Band		
548.2	18,242	Vibronic
550.6	18,162	1(c)-2(a)
555.2	18,012	1(c)-2(c)
557.7	17,931	1(a)-2(d)
561.2	17,819	1(b)-2(e)
(0, 0) Band		
578.4	17,289	0(a)-0(a)
(0, 1) Band		
588.1	17,004	0(a)-1(a)
589.4	16,966	0(a)-1(b)
591.9	16,895	0(a)-1(c)
(0, 2) Band		
610.1	16,391	0(a)-2(a)
612.8	16,319	0(a)-2(b)
615.7	16,242	0(a)-2(c)
617.5	16,194	0(a)-2(d)
621.5	16,090	0(a)-2(e)
(1, 4) Band		
626.5	15,962	1(c)-4(e)
635.2	15,743	1(a)-4(i)
(0, 3) Band		
646.5	15,468	0(a)-3(a)
648.8	15,413	0(a)-3(b)
652.3	15,330	0(a)-3(d)
655.0	15,267	0(a)-3(e)
656.6	15,230	0(a)-3(f)
660.0	15,152	0(a)-3(g)
(1, 5) Band		
668.0	14,970	
670.2	14,921	Not specified
(0, 4) Band		
689.0	14,513	0(a)-4(a)
693.7	14,415	0(a)-4(b)
697.5	14,337	0(a)-4(c)
702.0	14,245	0(a)-4(d)
705.2	14,180	0(a)-4(f)
709.1	14,102	0(a)-4(g)
710.1	14,082	0(a)-4(h)
713.8	14,010	0(a)-4(i)

Note. a, b, c, . . . , etc., are the Stark lines of ${}^5D_{0,1}$ or 7F_J ($J' = 0 \rightarrow 4$) as indicated.

TABLE V

SUMMARY OF THE 7F_J STARK LINES OBSERVED IN THE FLUORESCENCE SPECTRUM OF $\text{Eu}(\text{ReO}_4)_3 \cdot 2\text{DDPA}$

Transition (0, J')	Stark lines in C_3 symmetry ^a (Ref. (30))	No. of Stark lines observed	Oscillator strength ($f \times 10^6$)
(0, 0)	Γ_1	1	0.01
(0, 1)	$\Gamma_1 + 2\Gamma_2$	3	0.20
(0, 2)	$3\Gamma_1 + 2\Gamma_2$	5	1.10
(0, 3)	$3\Gamma_1 + 4\Gamma_2$	6	0.15
(0, 4)	$5\Gamma_1 + 4\Gamma_2$	9	0.12

^a In C_3 symmetry, each J -level splits into $(2J + 1)$ nondegenerate Stark lines characterized by Γ_1 (symmetric) and Γ_2 (antisymmetric) species (30).

dipole character, than the expected. The relative intensity distribution among the various J levels does not differ much following the rigorous selection rules (14, 27, 28). The oscillator strength data of Table V thus may be of interest at least for a qualitative comparison of their spectral characteristics. With this view, it is very interesting to visualize why the electric dipole intensity is more important for the ${}^5D_0 \rightarrow {}^7F_3$ transition than for the ${}^7F_0 \rightarrow {}^5D_3$ transition (it remains weaker (cf. Table I) than the even rigorously forbidden ${}^7F_0 \rightarrow {}^5D_0$ band out of the five absorptions to the 5D_J ($J = 0 \rightarrow 4$) manifold) while both follow the $\Delta J = \pm 3$ selection rule. The unusually large oscillator strength of the ${}^5D_0 \rightarrow {}^7F_3$ transition may be attributed to significant crystal-field-induced mixings of the 7F_3 state to components of the 7F_2 state, leading to the ${}^5D_0 \rightarrow {}^7F_2$ electric dipole strength being transferred into the transition (22).

The number of Stark lines observed for a given transition reflects the symmetry of the first-coordination sphere around the emitting ion (29). The (0, 0) transition of $\text{Eu}(\text{ReO}_4)_3 \cdot 2\text{DDPA}$ yields a single sharp band at $17,289 \text{ cm}^{-1}$ which cannot be split by any crystal field. Moreover, the energy levels of the 5D_0 , 5D_1 , and 7F_J manifold de-

duced by the results of ${}^7F_{0,1} \rightarrow {}^5D_{0,1}$ absorption and ${}^5D_{0,1} \rightarrow {}^7F_J$ emission are fairly consistent together. This certainly confirms that only one type of Eu(III) species is excited in this europium adduct (31). Forsberg (30) has given a detailed analysis of the Stark splitting of J multiplets. If the Eu(III) ion in the $\text{Eu}(\text{ReO}_4)_3 \cdot 2\text{DDPA}$ actually resides at a C_{2v} site symmetry as has been suggested by the previous authors (3), the Stark splitting would lead to one (0, 0), two (0, 1), four (0, 2), five (0, 3), and seven (0, 4) peaks. A comparison of the electronic

origins assigned in Tables IV and V reveals that the effective site symmetry for the Eu(III) can not be C_{2v} provided none of these bands is vibronic in nature. The possible symmetry that could account for the number of Stark lines observed is C_s . A possibility of C_2 symmetry for these features is not completely ruled out here. The fine structure of $(1, J')$ transitions (though all the Stark lines could not be resolved in each case) also suggests this symmetry.

The crystal-field levels splitant of the 7F_J multiplets deduced using the data of Table

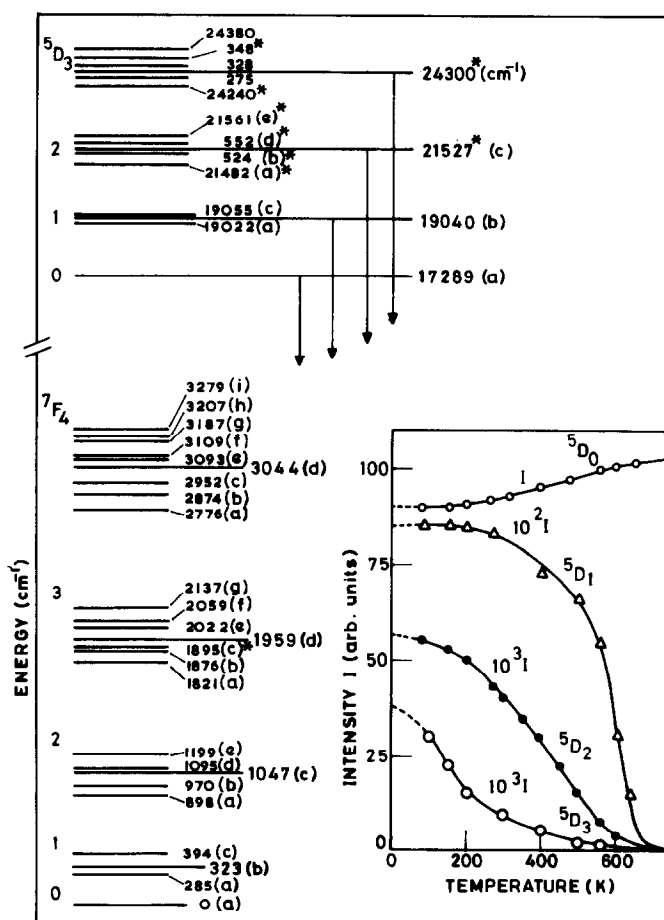


FIG. 5. Stark energy levels (not to scale) of the Eu(III) ion in $\text{Eu}(\text{ReO}_4)_3 \cdot 2\text{DDPA}$ at 77 K. (*) Data taken from absorption spectrum. The inset figure is the temperature variation of 5D_J ($J = 0 \rightarrow 3$) fluorescence intensity. The intensity scale on the vertical axis is given for 5D_0 fluorescence. This is to be multiplied by 10^{-2} and 10^{-3} , respectively, for the 5D_1 and ${}^5D_{2,3}$ fluorescence intensities.

IV are shown in Fig. 5. These provide the identification of electric dipole origins and their associated vibronic lines. Their energy and intensity distribution did not differ using different selective excitations. Emission from 5D_J ($J = 0 \rightarrow 3$) levels exhibited optimum intensity for the excitations made with 514.5, 488.0, 465.8, and 457.9 nm Ar^+ laser lines, respectively. None of the 5D_J crystal-field levels matches completely with any of these laser lines and the fluorescence in each case is induced through excitation of associated vibronic levels. The 5D_0 remains the prominent fluorescence state with all the excitations. A plot of the emission intensity variation of the various 5D_J states as a function of temperature is given in the inset of Fig. 5. The emissions originating from the 5D_3 , 5D_2 , and 5D_1 levels show a large decrease with increasing temperature. The rates at which the emission intensities decrease fall in the order ${}^5D_3 > {}^5D_2 > {}^5D_1$. On the other hand, the emission intensity from the 5D_0 state increases with increasing temperature. The higher ${}^5D_{J \geq 1}$ levels decay by a combination of the radiative (to ground state 7F_0) and nonradiative (to 5D_0) transitions. The nonradiative decay responsible for thermal quenching of the ${}^5D_{J \geq 1}$ states increases with temperatures and leads to population of the 5D_0 level, enhancing the fluorescence from the 5D_0 state at high (above ~ 300 K) temperatures.

Conclusions

The absorption and emission spectra of the $\text{Eu}(\text{III})$ ion in $\text{Eu}(\text{ReO}_4)_3 \cdot 2\text{DDPA}$ studied as a function of temperature allowed the assignment of the Stark levels of the various 7F_J , and 5D_J states. The $\text{Eu}(\text{III})$ ion in this adduct resides in a site symmetry characterized by C_2 point group. With increasing temperature (77 to 650 K), the fluorescence from ${}^5D_{J \geq 1}$ levels diminishes rapidly and increases from the 5D_0 level. This can be attributed to the decay of the ${}^5D_{J \geq 1}$ levels

by a combination of radiative and nonradiative transitions. The latter process dominates above 300 K with fluorescence occurring predominantly from the 5D_0 to various 7F_J levels.

Acknowledgments

The financial support from the CSIR is gratefully acknowledged. The authors thank Mr. R. K. Jain for his assistance in recording the spectra.

References

1. G. VICENTINI AND P. O. DUNSTAN, *J. Inorg. Nucl. Chem.* **34**, 1303 (1972).
2. G. VICENTINI, L. B. ZINNER, AND L. ROTHSCHILD, *Inorg. Chim. Acta* **9**, 213 (1974).
3. G. VICENTINI AND L. C. MACHADO, *J. Inorg. Nucl. Chem.* **43**, 1676 (1981).
4. G. BLASSE, *Phys. Status Solidi B* **55**, 131 (1973).
5. C. FOUASSIER, B. LATOURRETTE, J. PORTIER, AND P. HAGENMULLER, *Mater. Res. Bull.* **11**, 933 (1974).
6. W. A. SIBLEY AND N. KOUMVAKALIS, *Phys. Rev. B Condens. Matter* **14**, 35 (1976).
7. D. K. SARDAR, W. A. SIBLEY, AND R. ALCALA, *J. Lumin.* **27**, 401 (1982).
8. D. K. SARDAR, M. D. SHINN, AND W. A. SIBLEY, *Phys. Rev. B Condens. Matter* **26**, 2382 (1982).
9. R. REISFELD, M. EYAL, E. GREENBERG, AND C. K. JØRGENSEN, *Chem. Phys. Lett.* **118**, 25 (1985).
10. S. R. CHINN, H. Y. P. HONG, AND J. A. PIERCE, *Laser Focus* **12**, 64 (1976).
11. R. REISFELD AND C. K. JØRGENSEN, "Lasers and Excited States of Rare Earths," Springer-Verlag, New York (1979).
12. D. K. SARDAR AND R. C. POWELL, *J. Lumin.* **22**, 349 (1981).
13. W. T. CARNALL, P. R. FIELDS, AND K. RAJNAK, *J. Chem. Phys.* **49**, 4450 (1968).
14. A. F. KIRBY, D. FOSTER, AND F. S. RICHARDSON, *Chem. Phys. Lett.* **95**, 507 (1983).
15. S. RAM, J. S. YADAV, AND H. D. BIST, *Pramana* **22**, 17 (1984).
16. S. RAM, O. P. LAMBA, AND H. D. BIST, *Pramana* **23**, 59 (1984).
17. L. N. FEUERHELM, S. W. SIBLEY, AND W. A. SIBLEY, *J. Solid State Chem.* **54**, 164 (1984).
18. K. A. GSCHNEIDNER AND L. EYRING, "Handbook of Physics and Chemistry of Rare-Earths," Elsevier, Amsterdam/New York (1979).

19. M. L. SAGE, M. H. BUONOCORE, AND H. S. PINK, *Chem. Phys.* **36**, 171 (1979).
20. J. CHRYSOCHOOS, *J. Chem. Phys.* **60**, 1110 (1974).
21. S. RAM, O. P. LAMBA, AND J. S. YADAV, "Proceedings of Quantum Electronics," BARC Bombay, 1985, Vol. I, p. 189.
22. A. F. KIRBY AND F. S. RICHARDSON, *J. Phys. Chem.* **87**, 2544 (1983), and **87**, 2557 (1983).
23. G. HERZBERG, "Molecular Spectra and Molecular Structure," Vol. III, Van Nostrand, New York (1966).
24. J. C. DECIUS AND R. M. HEXTER, "Molecular Vibrations in Crystals," p. 326, McGraw-Hill, New York (1977).
25. D. L. KEPERT, *Proc. Inorg. Chem.* **23**, 1 (1977), and **24**, 179 (1978).
26. M. G. DREW, *Proc. Inorg. Chem.* **23**, 67 (1977).
27. G. S. OFELT, *J. Chem. Phys.* **37**, 511 (1962).
28. B. R. WYBOURNE, "Spectroscopic Properties of Rare Earths," Wiley, New York (1965).
29. J. CHRYSOCHOOS, P. W. M. JACOBS, AND M. J. STILLMAN, *J. Lumin.* **28**, 177 (1983).
30. J. H. FORSBERG, *Coord. Chem. Rev.* **10**, 195 (1973).
31. S. OIANG, C. BARTHOU, J. P. DENIS, F. PELLE, AND B. BLANZAT, *J. Lumin.* **28**, 1 (1983).